

# EphrinB2 is the entry receptor for Nipah virus, an emergent deadly paramyxovirus

Oscar A. Negrete<sup>1</sup>, Ernest L. Levroney<sup>1</sup>, Hector C. Aguilar<sup>1</sup>, Andrea Bertolotti-Ciarlet<sup>4</sup>, Ronen Nazarian<sup>1</sup>, Sara Tajyar<sup>1</sup> & Benhur Lee<sup>1,2,3</sup>

Nipah virus (NiV) is an emergent paramyxovirus that causes fatal encephalitis in up to 70 per cent of infected patients<sup>1</sup>, and there is evidence of human-to-human transmission<sup>2</sup>. Endothelial syncytia, comprised of multinucleated giant-endothelial cells, are frequently found in NiV infections, and are mediated by the fusion (F) and attachment (G) envelope glycoproteins. Identification of the receptor for this virus will shed light on the pathobiology of NiV infection, and spur the rational development of effective therapeutics. Here we report that ephrinB2, the membrane-bound ligand for the EphB class of receptor tyrosine kinases (RTKs)<sup>3</sup>, specifically binds to the attachment (G) glycoprotein of NiV. Soluble Fc-fusion proteins of ephrinB2, but not ephrinB1, effectively block NiV fusion and entry into permissive cell types. Moreover, transfection of ephrinB2 into non-permissive cells renders them permissive for NiV fusion and entry. EphrinB2 is expressed on endothelial cells and neurons<sup>3,4</sup>, which is consistent with the known cellular tropism for NiV<sup>5</sup>. Significantly, we find that NiV-envelope-mediated infection of microvascular endothelial cells and primary cortical rat neurons is inhibited by soluble ephrinB2, but not by the related ephrinB1 protein. Cumulatively, our data show that ephrinB2 is a functional receptor for NiV.

Emerging viral pathogens present a critical threat to global health and economies. NiV, and the related Hendra virus (HeV), are members of the newly defined Henipavirus genus of the *Paramyxoviridae* (refs 6,7), and are designated as priority pathogens in the National Institute of Allergy and Infectious Diseases' Biodefense Research Agenda. Since 1999, NiV outbreaks have occurred in Malaysia, Singapore and Bangladesh<sup>1,8</sup>, and have the potential to severely affect the pig-farming industry<sup>9</sup>.

NiV exhibits an unusually broad host range including humans, pigs, dogs, cats, horses, guinea pigs, hamsters and fruit bats (NiV's presumptive natural host)<sup>6,10,11</sup>. Such a broad range of host tropism is rare among extant paramyxoviruses. With the possible exception of fruit bats, the disease mortality of all other hosts has been established for both natural or experimental infection<sup>11,12</sup>. However, the mortality rate in pigs is less than 5% even though the transmission rate approaches 100% (refs 6,9), suggesting that zoonotic transmission to humans has increased the pathogenicity of the virus.

Endothelial cells are the major cellular targets for NiV, and hence syncytial endothelial cells in blood vessels are considered a characteristic feature of Nipah viral disease<sup>5</sup>. The fusion (F) and attachment (G) proteins of NiV mediate syncytia formation, and cell lines from many animal species are permissive for NiV-envelope-mediated fusion<sup>13,14</sup>, suggesting that the receptor for NiV is highly conserved.

To establish whether NiV-G determines the known cell line tropism of NiV, we generated an immunoadhesin by fusing the

ectodomain of NiV-G with the Fc region of human IgG1 (NiV-G-Fc). NiV-G-Fc bound to fusion-permissive 293T, HeLa and Vero cells<sup>13,15</sup>, but not to non-permissive Chinese hamster ovary (CHO-pgsA745), pig kidney fibroblast (PK13)<sup>13</sup> and human Raji B cells (Fig. 1a). NiV-G-Fc immunoprecipitated a 48 kDa band from the surfaces of permissive 293T and Vero cells, but not non-permissive CHO-pgsA745 cells (Fig. 1b). Analysis identified a deletion of 28 amino acids (see Supplementary Table 1) in the globular ectodomain of NiV-G, which is produced as an Fc-fusion dimer at wild-type levels, but no longer binds to the surfaces of permissive cells (Fig. 1b). This deletion mutant ( $\Delta$ 28NiV-G-Fc) was used as a negative control in preparative immunoprecipitation experiments to purify the putative NiV receptor. Parallel portions of the gel containing the 48 kDa band immunoprecipitated by NiV-G-Fc, but not by  $\Delta$ 28NiV-G-Fc, were analysed by trypsin digestion and mass spectrometry. Only one transmembrane protein was uniquely identified in the NiV-G-Fc sample versus the  $\Delta$ 28NiV-G-Fc sample. Two independent tryptic fragments of 12 and 17 amino acids each identified the protein as ephrinB2 (Supplementary Fig. 1).

EphrinB2 is essential for vasculogenesis and axonal guidance, and is expressed on endothelial cells, neurons and smooth muscle cells surrounding small arteries and arterioles<sup>16,17</sup>—an expression pattern

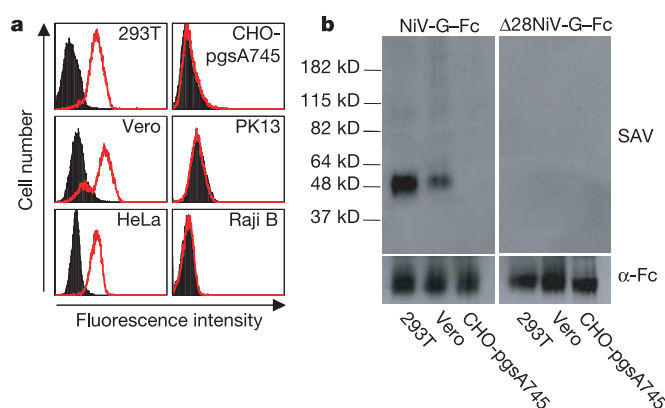


**Figure 1 | Soluble NiV-G binds to a 48 kDa membrane protein.** **a**, Equal amounts of NiV-G-Fc (thick line) or Fc-only (filled histogram) were incubated with permissive 293T, Vero or HeLa cells, or non-permissive CHO-pgsA745, PK13, or human Raji B cells. Cell-surface binding was detected by a phycoerythrin- (PE-) conjugated anti-human IgG secondary antibody. **b**, Cell surface proteins from permissive 293T and Vero cells, or non-permissive CHO-pgsA745 cells, were biotinylated, immunoprecipitated by NiV-G-Fc or  $\Delta$ 28NiV-G-Fc, run on a non-denaturing SDS-PAGE gel and detected by western blotting with HRP-conjugated streptavidin (SAV) or anti-human Fc ( $\alpha$ -Fc).

<sup>1</sup>Department of Microbiology, Immunology and Molecular Genetics, <sup>2</sup>Department of Pathology and Laboratory Medicine, <sup>3</sup>UCLA AIDS Institute, David Geffen School of Medicine, UCLA, Los Angeles, California 90095, USA. <sup>4</sup>Department of Microbiology, University of Pennsylvania, Philadelphia, Pennsylvania 19104, USA.

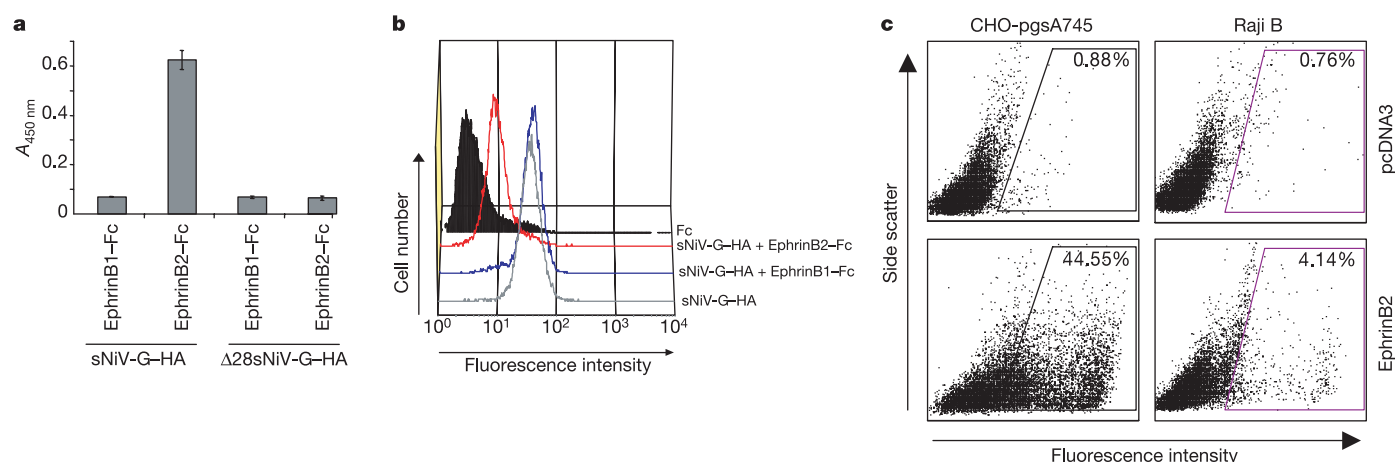


**Figure 2 | The ectodomain of NiV-G binds specifically to ephrinB2.** **a**, The soluble HA-tagged ectodomain of NiV-G (sNiV-G-HA) bound to ephrinB2-Fc but not ephrinB1-Fc in an ELISA (see Methods).  $\Delta 28\text{sNiV-G-HA}$ , with an identical deletion as in  $\Delta 28\text{NiV-G-HA}$ , did not bind to ephrinB2-Fc or ephrinB1-Fc.  $A_{450}$ , absorbance at 450 nm. One representative experiment out of three is shown. Data are averages of triplicates  $\pm$  s.d. **b**,  $10\ \mu\text{g ml}^{-1}$  of

ephrinB2-Fc but not ephrinB1-Fc was able to block sNiV-G-HA-binding to permissive 293T cells. sNiV-G-HA-binding was detected by a mouse monoclonal anti-HA antibody followed by a PE-conjugated anti-mouse IgG secondary antibody. **c**, NiV-G-Fc bound to ephrinB2-transfected but not to pcDNA3-transfected CHO-pgsA745 and human Raji B cells. Cell-surface binding was detected as in Fig. 1a.

highly concordant with the known cellular tropism of NiV<sup>5</sup>. Using a soluble HA-tagged ectodomain of NiV-G (sNiV-G-HA), we demonstrated that NiV-G bound directly to soluble ephrinB2-Fc, but not to ephrinB1-Fc, in an enzyme-linked immunosorbent assay (ELISA) (Fig. 2a). EphrinB1 is the most closely related ephrin to ephrinB2. Additionally, ephrinB2-Fc, but not ephrinB1-Fc, competed readily for sNiV-G-HA-binding on permissive 293T cells (Fig. 2b), and NiV-G-Fc bound to ephrinB2-transfected, but not to pcDNA3-transfected, CHO-pgsA745 and human Raji B cells (Fig. 2c). Cumulatively, these data demonstrate a direct and specific association between NiV-G and ephrinB2.

Because endothelial syncytia are a hallmark of NiV disease<sup>5</sup>, we

investigated whether ephrinB2 was required for NiV-envelope-mediated syncytia formation. We used a luciferase-reporter-based fusion assay driven by T7-polymerase that has been used extensively to examine viral-envelope-mediated cell-cell fusion<sup>18,19</sup>. NiV-F/G proteins mediated fusion with permissive 293T or Vero cells, but not with non-permissive PK13 or human Raji B cells (Fig. 3a). No fusion was seen in the absence of NiV-G. Again, soluble ephrinB2, but not ephrinB1, significantly inhibited NiV-F/G-mediated cell-cell fusion (Fig. 3b). Transfection of ephrinB2, but not ephrinB1 or green fluorescent protein (GFP), into human Raji B cells rendered them permissive for NiV-envelope-mediated fusion (Fig. 3c). This fusion was inhibited by soluble ephrinB2 or EphB4 (a cognate

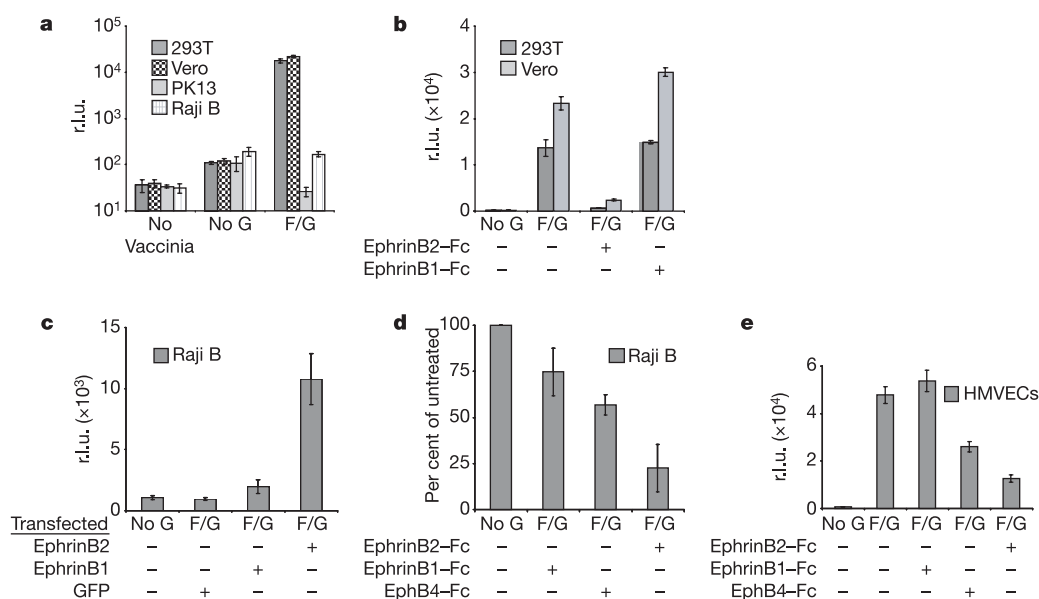


**Figure 3 | EphrinB2 is necessary for NiV fusion.** **a**, NiV-F/G-expressing 'effector' PK13 cells were placed on permissive (293T or Vero cells) or non-permissive (PK13 or human Raji B) 'target' cells and fusion quantified as described in Methods. **b**, Fusion assay was performed as in **a** for 293T and Vero cells except that ephrinB2-Fc or ephrinB1-Fc ( $10\ \mu\text{g ml}^{-1}$ ) was added to the target cells 30 min before addition of NiV-envelope-expressing effector cells. **c**, Fusion assay performed with transfected Raji B target cells

and PK13 effector cells. **d**, Inhibition studies on Raji B cells were performed as in **b** (EphB4-Fc:  $100\ \mu\text{g ml}^{-1}$ ). Fusion in each case was normalized to that obtained in the absence of any blocking reagent. **e**, Fusion assay between microvascular endothelial target cells and NiV envelope-expressing PK13 effector cells as described. Inhibition studies were performed as in **d**. Error bars indicate  $\pm$  s.d. from at least two independent experiments.

receptor for ephrinB2), but not ephrinB1 (Fig. 3d). Significantly, NiV-F/G-expressing cells also fused with human microvascular endothelial cells (HMVECs) in a manner that could be inhibited by soluble ephrinB2 or EphB4, but not ephrinB1 (Fig. 3e). Thus, NiV fusion on cell lines, and on an *in vivo* target cell for NiV infection, is dependent on ephrinB2.

Next we determined whether ephrinB2 could also mediate NiV infection. NiV is a Biosafety Level- (BSL-) 4 pathogen, so we developed a virion-based infection assay that does not require the use of a BSL-4 facility. Heterologous viral envelopes can be pseudotyped onto a recombinant vesicular stomatitis virus (VSV) expressing red fluorescent protein (RFP), but lacking its own envelope (VSV- $\Delta$ G-RFP)<sup>20</sup>. VSV- $\Delta$ G-RFP bearing the NiV-F/G proteins was used to infect permissive 293T or Vero cells, resulting in cells expressing RFP (Fig. 4a, b). Viral entry was dependent on NiV-F/G because it was neutralized by NiV-F/G-specific antiserum (Fig. 4a).

VSV-F/G-RFP infection was blocked by ephrinB2-Fc, but not ephrinB1-Fc, while infection by VSV-RFP bearing its own envelope (VSV-G) was not inhibited by either soluble ephrin (Fig. 4b).

Transfection of ephrinB2 into non-permissive CHO-pgsA745 cells rendered them permissive for viral entry (Fig. 4c). CHO-pgsA745 is a mutant CHO cell line that does not express cell surface heparan sulphate proteoglycans<sup>21</sup>. Heparan sulphate has been described as an attachment or entry receptor for many viruses, and may confound the search for bona fide viral receptors that mediate membrane fusion<sup>22</sup>. Thus, our observation that ephrinB2, in the absence of cell surface heparan sulphates, could mediate viral entry strongly suggests that ephrinB2 is a functional receptor for NiV entry. Finally, NiV-F/G-pseudotyped VSV was also able to infect primary cortical rat neurons and HMVECs (Fig. 4d, e)—two cell types that can be infected *in vivo*<sup>5</sup>. NiV-F/G infection of rat neurons and HMVECs was inhibited by soluble ephrinB2, but not ephrinB1. EphrinB2 inhibited

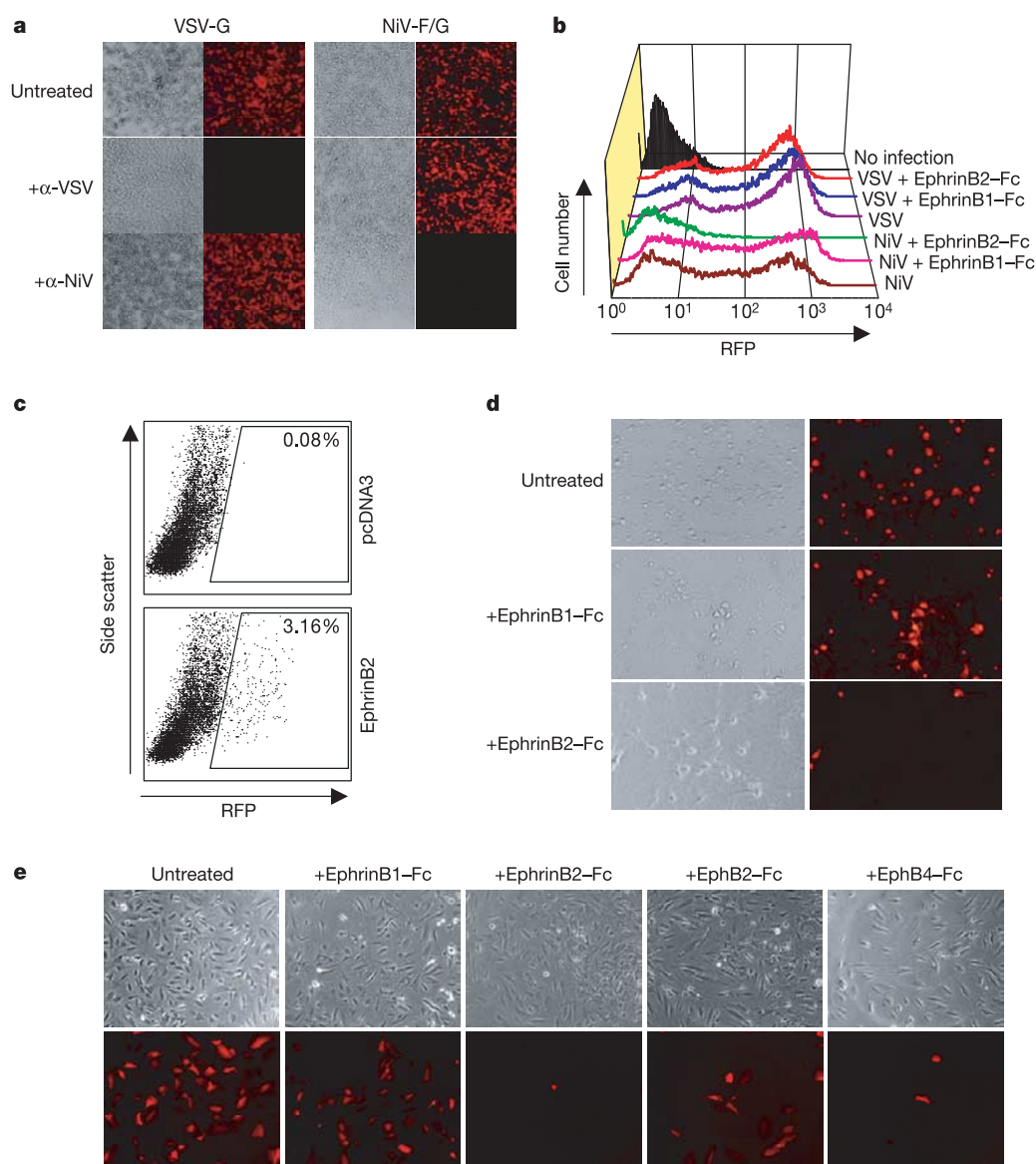


**Figure 4 | EphrinB2 mediates entry of NiV-F/G pseudotyped viruses.** **a**, VSV-G or NiV-F/G mediated entry into 293T cells was neutralized specifically by their respective antisera. Matched phase-contrast and fluorescent images are shown. **b**, NiV-F/G or VSV-G pseudotyped viruses were used to infect Vero cells in the presence or absence of ephrinB1-Fc or ephrinB2-Fc ( $10 \mu\text{g ml}^{-1}$ ). RFP production was analysed by FACS. **c**, Human ephrinB2- or pcDNA3-transfected CHO-pgsA745 cells were

infected with NiV-F/G pseudotyped VSV-RFP and FACS-analysed for RFP production. **d**, NiV-F/G pseudotyped VSV-RFP viruses were used to infect cortical rat neurons in the presence or absence of ephrinB1-Fc or ephrinB2-Fc ( $10 \mu\text{g ml}^{-1}$ ). Representative matched phase-contrast and fluorescent images are shown. **e**, Additional inhibition studies were performed with HMVECs (ephrinB1/B2-Fc,  $10 \mu\text{g ml}^{-1}$ ; EphB2/B4-Fc,  $100 \mu\text{g ml}^{-1}$ ).



NiV-F/G pseudotype infection of primary rat neurons by 76% compared to ephrinB1 (average number of infected cells per field  $\pm$  s.d.:  $5.7 \pm 4.3$  versus  $23.5 \pm 12.7$  for ephrinB2 versus ephrinB1 inhibition, respectively;  $P < 0.0001$ , Student's *t*-test). Additionally, we show that soluble EphB4 and EphB2 (the cognate receptors for ephrinB2) significantly inhibited NiV-F/G-mediated infection of HMVECs (Fig. 4e). Our use of HMVECs and primary rat neurons to show that NiV-envelope-mediated entry occurred in an ephrinB2-dependent manner strongly suggests that ephrinB2 is also a functional receptor for NiV entry *in vivo*.

In histopathological studies on patients who had succumbed to NiV infection, viral antigen can be detected in unequivocal amounts in relatively few cellular subtypes, such as neurons, endothelial cells and smooth muscle cells surrounding small arteries<sup>5</sup>. This is in concordance with the expression pattern of ephrinB2; in *lacZ* 'knock-in' mice, ephrinB2 was specifically expressed in endothelial cells, neurons and in smooth muscle cells surrounding arterioles<sup>16,17</sup>. The identification of ephrinB2 as the NiV receptor largely explains the *in vivo* tropism of the virus. EphrinB2 is a critical gene involved in embryogenic development, and has established roles in vasculogenesis and axonal guidance<sup>3,4</sup>. Ephrin genes are highly conserved and have been found in all animal species examined<sup>3</sup>. Thus, the conservation of ephrinB2 may also explain the unusually broad tropism of NiV. However, we note that not all cell lines are competent to express ephrinB2 well (our unpublished observations), and we have not conducted exhaustive gain-of-function experiments in all cell lines described to be non-permissive for NiV-envelope-mediated fusion<sup>13</sup>. Therefore, although ephrinB2 is clearly a functional receptor for NiV entry, it is possible that other factors in addition to ephrinB2 expression are required for productive NiV entry and replication.

Both ephrinB2 and its cognate receptor EphB4 have tyrosine signalling and PDZ (Postsynaptic density protein-95, Discs-large, Zonula occludens-1) binding motifs in their cytoplasmic domains<sup>23</sup>. 'Forward' signalling mediated by EphB4 facilitates anti-adhesive and repulsive behaviour upon contact with ephrinB2-expressing cells, while ephrinB2 'reverse' signalling facilitates propulsive adhesion upon contact with EphB4-expressing cells. If NiV-G acts like EphB4 and binds to ephrinB2, but lacks the property of reverse signalling, perhaps only forward propulsion will ensue. We speculate that this might act to recruit more endothelial cells to areas of NiV replication. Indeed, signalling-deficient EphB4 on tumour cells can promote invasion by ephrinB2-expressing endothelial cells<sup>24</sup>. It will be interesting to re-examine pathological specimens for increased angiogenesis in areas of NiV replication. It is also possible that PDZ binding domains, and other proteins known to interact with the cytoplasmic domain of ephrinB2, may play a role in the productive entry of NiV.

HeV appears to have a similar cellular tropism to NiV<sup>13</sup>, although NiV appears to be more pathogenic. Experiments are continuing to determine whether HeV also uses ephrinB2, or ephrinB2-related molecules, as its entry receptor. Discovery of ephrinB2 as the NiV receptor will facilitate screening of small-molecule antagonists to block NiV entry: molecules targeting NiV-G may be potential antivirals, whereas molecules targeting ephrinB2 may have applications in the field of angiogenesis. The recent and repeated outbreaks of NiV in Bangladesh<sup>1</sup> emphasize the importance of the search for vaccines and therapeutics against this emerging pathogen. Identifying the NiV receptor will contribute to these continuing efforts.

## METHODS

**Cells and reagents.** Primary rat cortical neurons were dissected and cultured from embryonic day 17 Sprague-Dawley rats as described<sup>25</sup>, and plated 2 weeks before infection. HMVECs immortalized with the human telomerase catalytic protein (hTERT)<sup>26</sup> were a gift from R. Shao. Soluble Fc-fusion proteins of ephrins and Eph receptors were obtained from R&D Systems. Sequence-verified human ephrinB2 clones were obtained from Origene (CMV-driven clones) and Open Biosystems (T7-driven clones). The open reading frame of

human ephrinB2 was also subcloned into pcDNA3 (Invitrogen) in frame with a C-terminal V5 epitope tag.

**Identification of NiV-ephrinB2 interaction.** See Supplementary Methods 1 for details of soluble NiV-G production. 293T, Vero or CHO-pgsA745 cells were cell-surface biotinylated using EZ-link Sulfo-NHS-LC-LC-Biotin reagent (Pierce). Each 100-mm dish of cells was lysed (50 mM Tris-HCl, 150 mM NaCl, and 1% Triton X-100, pH 8.0 with protease inhibitors), clarified by centrifugation and pre-cleared by one round of mock immunoprecipitation with Fc-only protein using protein G-coupled magnetic beads (Dyna). Pre-cleared lysates were immunoprecipitated with NiV-G-Fc or  $\Delta$ 28NiV-G-Fc previously crosslinked to protein G beads (20 mM dimethyl-pimelimidate-HCl in 0.2 M triethanolamine) (Sigma), separated by non-denaturing SDS-polyacrylamide gel electrophoresis (SDS-PAGE) and analysed by western blotting with horseradish peroxidase- (HRP-) conjugated streptavidin or anti-human Fc (Pierce). 293T cells ( $3 \times 10^7$ ) were used for preparative immunoprecipitations, and proteins were visualized using Silver Stain Plus (BioRad). Parallel portions of the gel containing a specific band immunoprecipitated by NiV-G-Fc, but not  $\Delta$ 28NiV-G-Fc, were excised, digested in the gel with sequencing-grade trypsin and subjected to peptide sequencing by tandem mass spectrometry (MS/MS). A Finnigan ion trap mass spectrometer LCQ coupled with a high-performance liquid chromatography (HPLC) system running a 75- $\mu$ m inner diameter C18 column was used. MS/MS spectra were used to search the most recent non-redundant protein database from GenBank with the ProtQuest software suite (ProtTech).

**Fusion assay.** Fusion assays were performed essentially as described<sup>18,19</sup>. Briefly, effector cells (PK13) were transfected with 0.3  $\mu$ g of codon-optimized NiV-F and G expression plasmids, 0.6  $\mu$ g of T7-luciferase, and 0.8  $\mu$ g of pcDNA3 per 6-well plate using Lipofectamine 2000 reagent (Invitrogen). The sequences of the codon-optimized genes have been deposited into GenBank (AY816748 and AY816746 for F and G, respectively, based on the original sequences described for NiV-F and -G in ref. 6.). The DNA amount was always kept constant with pcDNA3. Target cells (293T, Vero, HMVECs) grown in a 24-well plate were infected with vaccinia virus (vTF1.1) expressing T7-polymerase (multiplicity of infection, MOI = 5), and cultured overnight in DMEM 10% FCS. Rifampicin was added to reduce cytopathicity. Effector cells ( $1 \times 10^5$ ) were mixed with target cells in a total volume of 250  $\mu$ l, allowed to fuse for 6 h and then lysed with 180  $\mu$ l of lysis buffer (20 mM Tris pH 7.5, 100 mM  $\text{NH}_4\text{SO}_4$ , 0.1% BSA, 0.75% Triton X-100, and 0.001% sodium azide). Luciferase activity was detected by adding equal volumes (100  $\mu$ l) of luciferase detection reagent (Promega) and lysate, and the relative light units (r.l.u.) were determined by luminometry. When Raji B cells were used as target cells,  $2.5 \times 10^6$  cells were transfected with 6  $\mu$ g of the indicated plasmid using Amaxa's Nucleofector electroporation device for transfection in buffer V or T on program A23. These suspension target cells were added onto the adherent PK13 effector cells prepared as described. Fusion was analysed as above.

**Binding of soluble NiV-G to ephrinB2.** 3  $\mu$ g ml<sup>-1</sup> of ephrinB1-Fc and ephrinB2-Fc diluted in ELISA buffer (2% BSA and 0.05% Tween-20 in TBS) were captured by biotinylated anti-human Fc (Caltag) pre-bound to NeutrAvidin-coated polystyrene plates (Pierce). Supernatant from sNiV-G-HA- or  $\Delta$ 28sNiV-G-HA-transfected 293T cells was added to each well, and detected with an HRP-conjugated anti-HA antibody (Novus Biologicals) using TMB substrate (Pierce).

**Infection assay.** The VSV- $\Delta$ G-RFP virus is a recombinant VSV derived from a full-length complementary DNA clone of the VSV Indiana serotype in which the G-protein gene has been replaced with the RFP gene<sup>20</sup> (a gift from M. Whitt). Either VSV-G or NiV-F/G was provided *in trans*. NiV-F/G and VSV-G pseudotypes were purified via centrifugation through a sucrose cushion and used to infect 293T, Vero, CHO-pgsA745, rat cortical neurons and HMVECs (MOI = 1, as titred on 293T cells). RFP production at 24 h was analysed by fluorescent microscopy or FACS.

**Neutralization sera.** For NiV, New Zealand White rabbits were genetically immunized with a mixture of codon-optimized NiV-M (matrix), NiV-F and NiV-G expression plasmids (Aldevron) using an electroporation protocol that results in increased antibody titres<sup>27</sup>. A 1:100 dilution of hyperimmune sera from the terminal bleed was used for neutralization studies. For VSV, a VSV-G-specific mouse monoclonal antibody (clone 8G5F II, a gift from J. Rose) was used. Pseudotyped viruses were pre-incubated with antibodies for 1 h before use for infection.

Received 18 March; accepted 17 May 2005.

Published online 6 July 2005.

1. Hsu, V. P. *et al.* Nipah virus encephalitis reemergence, Bangladesh. *Emerg. Infect. Dis.* 10, 2082–2087 (2004).

2. The International Centre for Diarrhoeal Disease Research, Bangladesh (ICDDRDB). Person-to-person transmission of Nipah virus during outbreak in Faridpur District. *Health Sci. Bull.* **2**, 5–9 (2004).
3. Poliakov, A., Cotrina, M. & Wilkinson, D. G. Diverse roles of eph receptors and ephrins in the regulation of cell migration and tissue assembly. *Dev. Cell* **7**, 465–480 (2004).
4. Palmer, A. & Klein, R. Multiple roles of ephrins in morphogenesis, neuronal networking, and brain function. *Genes Dev.* **17**, 1429–1450 (2003).
5. Wong, K. T. *et al.* Nipah virus infection: pathology and pathogenesis of an emerging paramyxoviral zoonosis. *Am. J. Pathol.* **161**, 2153–2167 (2002).
6. Chua, K. B. *et al.* Nipah virus: a recently emergent deadly paramyxovirus. *Science* **288**, 1432–1435 (2000).
7. Harcourt, B. H. *et al.* Molecular characterization of Nipah virus, a newly emergent paramyxovirus. *Virology* **271**, 334–349 (2000).
8. Parashar, U. D. *et al.* Case-control study of risk factors for human infection with a new zoonotic paramyxovirus, Nipah virus, during a 1998–1999 outbreak of severe encephalitis in Malaysia. *J. Infect. Dis.* **181**, 1755–1759 (2000).
9. Lam, S. K. Nipah virus—a potential agent of bioterrorism? *Antiviral Res.* **57**, 113–119 (2003).
10. Field, H. *et al.* The natural history of Hendra and Nipah viruses. *Microbes Infect.* **3**, 307–314 (2001).
11. Wong, K. T. *et al.* A golden hamster model for human acute Nipah virus infection. *Am. J. Pathol.* **163**, 2127–2137 (2003).
12. Hooper, P., Zaki, S., Daniels, P. & Middleton, D. Comparative pathology of the diseases caused by Hendra and Nipah viruses. *Microbes Infect.* **3**, 315–322 (2001).
13. Bossart, K. N. *et al.* Membrane fusion tropism and heterotypic functional activities of the Nipah virus and Hendra virus envelope glycoproteins. *J. Virol.* **76**, 11186–11198 (2002).
14. Tamin, A. *et al.* Functional properties of the fusion and attachment glycoproteins of Nipah virus. *Virology* **296**, 190–200 (2002).
15. Guillaume, V. *et al.* Nipah virus: vaccination and passive protection studies in a hamster model. *J. Virol.* **78**, 834–840 (2004).
16. Gale, N. W. *et al.* Ephrin-B2 selectively marks arterial vessels and neovascularization sites in the adult, with expression in both endothelial and smooth-muscle cells. *Dev. Biol.* **230**, 151–160 (2001).
17. Shin, D. *et al.* Expression of ephrinB2 identifies a stable genetic difference between arterial and venous vascular smooth muscle as well as endothelial cells, and marks subsets of microvessels at sites of adult neovascularization. *Dev. Biol.* **230**, 139–150 (2001).
18. Rucker, J. *et al.* Cell-cell fusion assay to study role of chemokine receptors in human immunodeficiency virus type 1 entry. *Methods Enzymol.* **288**, 118–133 (1997).
19. Bossart, K. N. & Broder, C. C. Viral glycoprotein-mediated cell fusion assays using vaccinia virus vectors. *Methods Mol. Biol.* **269**, 309–332 (2004).
20. Takada, A. *et al.* A system for functional analysis of Ebola virus glycoprotein. *Proc. Natl Acad. Sci. USA* **94**, 14764–14769 (1997).
21. Esko, J. D., Stewart, T. E. & Taylor, W. H. Animal cell mutants defective in glycosaminoglycan biosynthesis. *Proc. Natl Acad. Sci. USA* **82**, 3197–3201 (1985).
22. Liu, J. & Thorp, S. C. Cell surface heparan sulfate and its roles in assisting viral infections. *Med. Res. Rev.* **22**, 1–25 (2002).
23. Kullander, K. & Klein, R. Mechanisms and functions of Eph and ephrin signalling. *Nature Rev. Mol. Cell Biol.* **3**, 475–486 (2002).
24. Noren, N. K., Lu, M., Freeman, A. L., Koolpe, M. & Pasquale, E. B. Interplay between EphB4 on tumour cells and vascular ephrin-B2 regulates tumour growth. *Proc. Natl Acad. Sci. USA* **101**, 5583–5588 (2004).
25. Estus, S. *et al.* Aggregated amyloid-beta protein induces cortical neuronal apoptosis and concomitant “apoptotic” pattern of gene induction. *J. Neurosci.* **17**, 7736–7745 (1997).
26. Shao, R. & Guo, X. Human microvascular endothelial cells immortalized with human telomerase catalytic protein: a model for the study of *in vitro* angiogenesis. *Biochem. Biophys. Res. Commun.* **321**, 788–794 (2004).
27. Tollefsen, S. *et al.* DNA injection in combination with electroporation: a novel method for vaccination of farmed ruminants. *Scand. J. Immunol.* **57**, 229–238 (2003).

**Supplementary Information** is linked to the online version of the paper at [www.nature.com/nature](http://www.nature.com/nature).

**Acknowledgements** We thank M. Whitt for permission to use the VSV-pseudotype system, B. Reversade for discussions, and K. Adams for editorial comments. This work was supported by NIH grants to B.L., an NIH NRSA grant to O.A.N., an emerging infectious disease training grant to A.B.-C., and a biodefence research fellowship to E.L.L. S.T. was supported by an NSF-funded UCLA-IGERT bioinformatics traineeship. B.L. is a recipient of the Burroughs Wellcome Fund Career Development Award and is also a Charles E. Culpepper Medical Scholar supported by the Rockefeller Brothers Fund and by Goldman Philanthropic Partnerships. We also acknowledge support from the UCLA AIDS Institute and the flow cytometry core (UCLA CFAR).

**Author Contributions** E.L.L., H.C.A., A.B.-C. and R.N. contributed equally to this work.

**Author Information** Reprints and permissions information is available at [npg.nature.com/reprintsandpermissions](http://npg.nature.com/reprintsandpermissions). The authors declare no competing financial interests. Correspondence and requests for materials should be addressed to B.L. ([bleebhl@ucla.edu](mailto:bleebhl@ucla.edu)).